Abstract. We have developed a new evolutionary synthesis code, which incorporates the output from chemical evolution models. We compare results of this new code with other published codes, and we apply it to the irregular galaxy NGC 1560 using sophisticated chemical evolution models. The code makes important contributions in two areas: a) the building of synthetic populations with time-dependent star formation rates and stellar populations of different metallicities; b) the extension of the set of stellar tracks from the Geneva group by adding the AGB phases for $m_i/M_\odot \geq 0.8$ as well as the very low mass stars. Our code predicts spectra, broad band colors, and Lick indices by using a spectra library, which cover a more complete grid of stellar parameters. The application of the code with the chemical models to the galaxy NGC 1560 constrain the star formation age for its stellar population around 10.0 Gy.

SPECTRAL: New Evolutionary Synthesis code. An application to the irregular galaxy NGC 1560

Gerardo A. Vázquez[1], Leticia Carigi[1], & J. J. González[1]

Instituto de Astronomía, Universidad Nacional Autónoma de México, A.P. 70-264, D.F. 04510, México
email: gerar, carigi, jesus@astroscu.unam.mx

1. Introduction

The study of the history of the evolution of galaxies includes three important issues: *spectral*, *dynamical*, and *chemical evolution*. Since these three different parts of the galaxy evolution are very difficult to study in simple models. Different authors has been focused to one of these parts. Although several efforts have been devoted by different authors (for example Tinsley 1972 and Vazdekis (1996)) to build complete spectro-chemical evolution codes. It has been difficult to incorporate the new releases in stellar models (structure evolution, stellar yields and stellar atmospheres) to the complexity of galaxy evolution models. The last reason has resulted in the division of the study of the spectro-chemical galaxy evolution in two complementary ways. While the chemical evolution models are the independent variable in the complete spectro-chemical evolution, the spectral evolution codes, which use population synthesis or evolutionary synthesis are left to use simple star formation histories to constrain the results and to be independent models.

In this way, we find sophisticated chemical evolution models. But, the most part of spectral evolution models consider the star formation in a simple star-burst, and a complicated star formation history can be modeled by many star-bursts of different metallicities and star formation rates. Thus, instead of studying a broad range of galaxies using simple star-burst models, it is preferable to develop spectro-chemical evolution models of neighboring galaxies using constrains to model the systems, and after that use the models to galaxies at higher red-shifts.

The new code (SPECTRAL) presented here has two important contributions to the evolutionary synthesis models: the first one is the consideration of a more complete set of evolutionary tracks from the Geneva group, adding tracks from Chabrier & Baraffe (1997) to the very low mass range; the second one is the construction of synthetic populations following the chemical evolution model in order to derive the spectral properties for systems with arbitrary enrichment history.

Send offprint requests to: Gerardo A. Vázquez

In this paper we initially use simple star formation scenarios to test the new evolutionary synthesis code, and then we proceed to more complete chemical evolution models to constrain the age of stellar population in the irregular galaxy NGC 1560.

In Section 2 we illustrate how the tracks are assembled to built a complete set of tracks for either the high mass loss rates, or the normal mass loss rates, and we describe the spectra library used in our code. In Section 3, we describe the process followed to built the evolutionary synthesis code, and the transformation to the observational plane of the variables. In Section 4 we test and compare SPECTRAL with others codes commonly used in the field and we present a first application by predicting spectral variables for the irregular galaxy NGC 1560. Finally, we discuss our conclusions.

2. Stellar Tracks

We have incorporated all the tracks from the Geneva group: Schaller et al. (1992, I), Schaerer et al. (1993a, II), Charbonnel et al. (1993, III), Schaerer et al. (1993b, IV), Meynet et al. (1994, V), Charbonnel et al. (1996, VI), Mowlavi et al. (1998, VII) and Charbonnel et al. (1999, VIII); together with tracks from Chabrier & Baraffe (1997, CB) for the very low mass stars, in order to assemble a complete dual grid of evolutionary tracks for the spectral code. One set with higher stellar mass loss and the other with normal mass loss as showed in Table 1. **All these tracks are published in such way that each evolutionary point over each track has an equivalent evolutionary point in the rest of the tracks** except for tracks from CB. This can be seen from the first line in the Table 1 because the tracks have the same number of evolutionary points (51). This is a very important aspect, because it is the basis of our evolutionary synthesis code.

We have chosen tracks with overshooting to be assembled by using linear and bilinear logarithmic interpolation when it is possible and the final result is shown in Table 2. The process to assemble the tracks is described below, and all parameters are logarithmic.

Table 1. Ingredients of the assemble of tracks.

Tracks Group	Phases	Points	Low Mass	High Mass	Metalli- cities
I, II III, IV	MS, RGB, HB[1], AGB[1]	51	0.8	120.0	a
V	MS, RGB, HB, AGB	51	12.0	120.0	b
VI	MS, RGB, HB, AGB	54	0.8	1.7	c
VII	MS, RGB, HB[1], AGB[1]	51	0.8	60.0	d
VIII	MS, RGB,	51	0.4	1.0	e
CB	PMS, MS,	4	0.075	0.8	f

a $Z = 0.001, 0.004, 0.008, 0.02, 0.04$ & $\dot{M} \propto Z^{0.5}$
b $Z = 0.001, 0.004, 0.008, 0.02, 0.04$ & $\dot{M} \propto 5.0 \times Z^{0.5}$
c $Z = 0.001, 0.02$ & $\dot{M} \propto Z^{0.5}$
d $Z = 0.1$ & $\dot{M} \propto Z^{0.5}$
e $Z = 0.001, 0.02$ & $\dot{M} \propto Z^{0.5}$
f $Z = 0.0002, 0.00063, 0.001, 0.002, 0.0063, 0.02$ & $\dot{M} = 0$
[1]Only for stars $m_i/M_\odot > 1.7$

Table 2. Main features from the new set of tracks.

Tracks Group	Phases	Points	Low Mass	High Mass	Metalli cities
Geneva + Lyon	PMS- AGB[1]	84	0.08	120.0	a
Geneva + Lyon	PMS- AGB[1]	84	0.08	120.0	b

a $Z = 0.001, 0.004, 0.008, 0.02, 0.04, 0.1$ & $\dot{M} \propto Z^{0.5}$
b $Z = 0.001, 0.004, 0.008, 0.02, 0.04$ & $\dot{M} \propto 5.0 \times Z^{0.5}$
[1]PMS-AGB means PMS, MS, RGB[2], HB[2], AGB[2]
[2]Only for stars $m_i/M_\odot > 0.7$

First of all, we completed phases covered at each metallicity. This means that tracks, which do not have post-main sequence evolution for masses in the range $m_i/M_\odot \leq 1.7$ (m_i is the initial mass, mass on main sequence) were completed to get 51 evolutionary points covering phases from the post-main sequence RGB, HB, and AGB.

We have used a IDL code to visualize each interpolation in tracks, using weights for linear interpolations defined:

$$wf_1 = \frac{(f_x - f_{j-1})}{(f_j - f_{j-1})}, \quad wf_0 = 1.0 - wf_1, \tag{1}$$

where f_x is the desired variable for which the properties are calculated when we interpolate in mass, metallicity or evolutionary phase. The sub-indices mean adjacent variables in tracks for the interpolation. New variables (V) were calculated using the equation:

$$V(f) = V(f_{j-1}) \times wf_0 + V(f_j) \times wf_1. \tag{2}$$

Phases beyond RGB were not present for stars in the mass range $1.0 \leq m_i/M_\odot \leq 1.7$, and post-main sequence phases were not present for stars in $0.8 \leq m_i/M_\odot < 1.0$ at some metallicities. The first step in the new set of tracks was to complete tracks up to RGB for those masses in $0.8 \leq m_i/M_\odot \leq 1.7$ using the last equations.

The second step was to add phases as HB and AGB for the range in masses $0.8 \leq m_i/M_\odot \leq 1.7$. To do the interpolation and extrapolation in this phases we used tracks from two sets at metallicities $Z = 0.001$ and 0.02 mentioned in the tracks group VI in Table 1. In this way, it was necessary to interpolate and extrapolate this phases

in metallicity. We followed in this part the shape of tracks in groups I, II, III, IV, and VII for the RGB to add the other two phases HB and AGB in the next form:

We completed the evolutionary points for the RGB in the tracks group VI up to 30 instead of original 3 using the fact that luminosity grows in this phase linearly as explained in I. We did the same for the rest of tracks for masses $m_i/M_\odot \geq 1.7$ in groups I, II, III, IV, and VII to get 81 evolutionary points for tracks instead of 51 in the first group.

Furthermore, to interpolate and extrapolate the post-RGB phases for the rest groups in metallicity we use the next method:

The metallicity against the shape of each stellar variable (age, $current\ mass$ (m_c), $L/L_\odot$, and T_{eff}) is fitted for linear functions $f_1(Z)$ and $f_2(Z)$ for both groups of tracks I, II, III, IV, VII, and VI, respectively, by using the metallicities at which both groups coincide, in this case $Z = 0.001$ and 0.02.

Then, we defined $Q(Z) = f_1(Z)/f_2(Z)$, as the factor to convert the shape of $f_1(Z)$ in to $f_2(Z)$ shape, or vice versa. Actually, we used the last point in RGB for the first tracks group as the first point in the new set of tracks and we interpolate in metallicity $\Delta(age)$, $\Delta(m_c)$, $\Delta(L/L_\odot)$, $\Delta(T_{eff})$ from the second group of tracks with the last method. Then, the second point in the new set of tracks is the last point in the RGB plus the first Δ interpolated, and so on.

The final step to assemble the tracks was to incorporate the very low mass stars by using models from CB. An interpolation in metallicity has been done to put these tracks as the same metallicities than Geneva tracks. Then, we have identified over the four evolutionary points of tracks, ZAMS points and pre-main sequence points to obtain in the full new set of tracks 84 equivalent evolutionary points from pre-main sequence up to AGB.

For comparison we show in the Figure 1 and Figure 2 Geneva tracks and the new set of tracks with new phases, and new stellar tracks for very low masses with normal mass loss rate, respectively.

We can see in Figure 2 the pre-main sequence phases included for masses $m_i/M_\odot \leq 0.7$. In the same way, tracks for $Z = 0.1$ are very poorly interpolated because these tracks are originally incomplete, and have been completed with tracks with $Z = 0.04$ for masses $m_i/M_\odot > 60$. Finally, it has been obtained two homogeneous grids to interpolate the stellar variables in time, mass, and metallicity either, one with normal mass loss ($\dot{M} \propto Z^{0.5}$) and second one using tracks from the V group for masses in the range $12.0 \leq m_i/M_\odot \leq 120.0$ in the Table 1 with high mass loss ($\dot{M} \propto 5 \times Z^{0.5}$), and stars in the range of $m_i/M_\odot < 12.0$ completed in the same way as the set with normal mass loss showed in Figure 2.
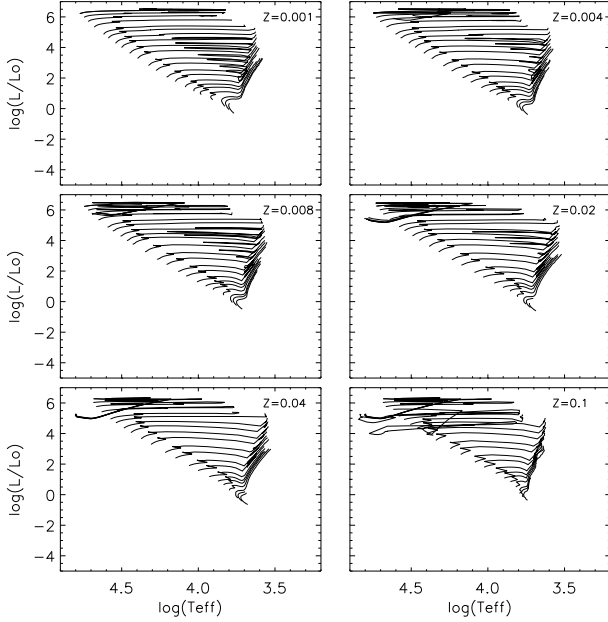
3. The Evolutionary Synthesis Code SPECTRAL

Fig. 1. $\mathrm{Log}(T_{eff})$ vs. $\log(L/L_\odot)$. Tracks I, II, III, IV, and VII from Geneva group, for masses 0.8 - 120.0 $\mathrm{M}_\odot$.
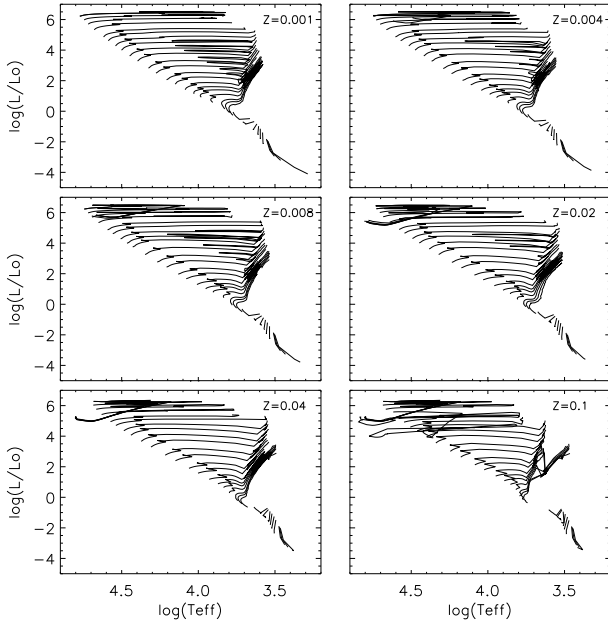

Fig. 2. $\mathrm{Log}(T_{eff})$ vs $\log(L/L_\odot)$. New sets, of tracks, for masses 0.08 - 120.0 $\mathrm{M}_\odot$.

3.1. The Input and Synthetic Stellar Populations

The evolutionary synthesis code has been developed in such away that it is possible to use the output of chemical evolution models taking from these models the following parameters:

-Duration of star formation, t_{SFH}.
-Star Formation Rate, $\Psi(t)$.

-Metallicity of interstellar gas at time t, $Z(t)$.

The code needs the number of stars $n(m_i, t)$ formed at any time in the interval $m_l \leq m_i/M_\odot \leq m_h$ defined as follows:

$$n(m_i, t) = \Phi(m_i)\Psi(t) \tag{3}$$

where m_l, m_h are the limits in mass and $\Phi(m_i)$ is the initial mass function.

$Z(t)$ is the metallicity of gas at which a new stellar population is born. Therefore, the new stars have a different metallicity or at least equal, predicted by the chemical evolution model.

When we see the synthetic stellar population formed over the whole continuous star formation history from $t = 0$ up to t_{SFH} at Age of 10.0 Gy for instance, we need to calculate how many stars are still alive since they have formed in each step of time with the SFR (in this case those stars in the tip of AGB). If $t_{SFH} = Age$ then the result of this procedure is that most of the stars formed in the first generation have died after 10.0 Gy, and just the very low mass stars are alive. The last generation formed at 10.0 Gy is complete and the age for this population (A_s) is zero. This means:

$$A_s = Age - t \tag{4}$$

where t runs from 0.0 up to t_{SFH} which could be the same as Age.

The final result at 10.0 Gy is a mix of populations after the chemical evolution has regulated the SF.

One of the problems in the evolutionary synthesis codes is the oscillations in the evolution of spectral parameters, because the post main sequence phases are not well sampled, due to the faster evolution of stars after the hydrogen burning phase. As shown in the Section 2, the problem is solved by interpolating in phases (evolutionary points) over the post hydrogen burning evolution, and interpolating in time and mass over main sequence phases.

To calculate which stars are alive at Age in the post-main sequence region, we first calculate the masses of stars at each evolutionary points since the turn off point up to AGB using relations $ta(Z, m_i, j)$ vs m_i (where ta is the age of each evolutionary point j over each track and initial mass m_i). If those ages satisfy the condition

$$ta(Z, m_i, j) \leq A_s \leq ta(Z, m_i, j + 1), \tag{5}$$

this means, 70 ages every time step, which cover exactly important post-main sequence evolutionary phases. The interpolation in phases is extended to metallicity using equation (1) and (2) to obtain:

$$ta(Z, m_i, j) = ta(Z_0, m_i, j) \times wZ_0 + \\ ta(Z_1, m_i, j) \times wZ_1, \tag{6}$$

which represents the age of each 70 evolutionary points ta, at required metallicity for all masses in tracks m_i. Masses at each 70 evolutionary points at required A_s are calculated using equation (1) for the time $ta(Z, m_i)$ in the following way:

$$m_i(Z, ta) = m_i(Z, m_{i_0}, ta) \times wt_0 + \\ m_i(Z, m_{i_1}, ta) \times wt_1 \tag{7}$$

where weights in time (wt_0 y wt_1) use $ta(Z, m_i, j)$ and A_S.

Table 3. Features of SED's and broad band colors calibration used in this work.

Para-meters	Lejeune et al. (1997, 1998)
T_{eff} (K)	$(2000, 50000)$ K
$\log g$	$(-1.02, 5.5)$
$[M/H]$	$(-5.0, 1.0)$
$\lambda\lambda$ (nm)	$(9.1, 160000)$
$n(\Delta\lambda)$	1221
Colors	14

To sample those masses in main sequence and pre-main sequence phases, we divide the mass range $m_l \leq m_i \leq m_{Toff}$, where m_{Toff} is the mass in the turn off point, in 80 masses to get a 150 masses for the synthetic population for each time step of evolution.

Once obtained this masses, we can calculate the stellar properties like m_c, $L/L_\odot$, T_{eff} interpolating in time, mass, and metallicity by using the equations (1) and (2) shown in Section 2.

3.2. Transformation from theoretical to observational plane

The stellar parameters in the synthetic population are transformed to the observable parameters by using the calibration of Lejeune et al. (1997), and Lejeune et al. (1998) which includes low resolution spectral energy distribution's (SED's) and broad band colors. Table 3 shows the grid of parameters covered by this library.

Following the same procedure as in tracks, we interpolate linearly over this grid using the same equations described in the Section 2, but now for $[M/H]$, T_{eff}, and $log(g)$ (gravity), where $[M/H] = log(Z/Z_\odot)$, with $Z_\odot = 0.02$. Besides the spectrum, and broad band colors, we have included the Lick indices Worthey et al. (1994) using the routine developed by J.J. Gonzalez in González (1993).

To integrate the observable variables for all alive stars we have to transforms in light or flux those variables given in magnitudes like colors and indices. In this way, we use the formalism described in González (1993) to integrate the Lick indices, and

$$L_{f_1} = L_{f_0} \times 10^{-0.4 \times (f_1 - f_0)}, \tag{8}$$

where f_1 can be the V filter, and f_0 the bolometric correction, for instance, and we follow the same procedure for the rest of filters using the rest of colors.

The spectral variables are weighted by the star number and the average values are:

$$< L_f > = \frac{\int_0^{Age} \int_{m_l}^{m(t)} L_f(Z, m', t')\, w(m', t')\, dm'\, dt'}{\int_0^{Age} \int_{m_l}^{m(t)} w(m', t')\, dm'\, dt'} \tag{9}$$

where the weights to obtain the average are defined

$$w(m', t') = \begin{cases} n(m', t') \times F_C & \text{For indices} \\ n(m', t') \times L_{bol} & \text{For colors} \\ n(m', t') & \text{For spectra,} \end{cases} \tag{10}$$
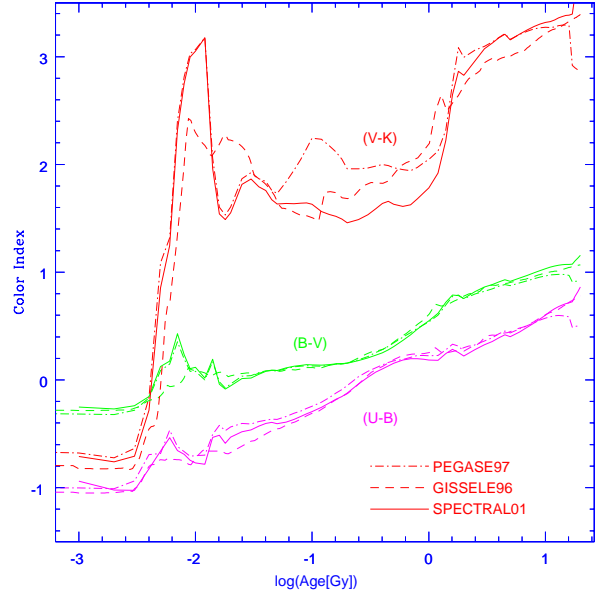
Fig. 3. Predicted color index evolution of star-burst at $Z_\odot$ by three different codes; PEGASE97, GISSEL96, and SPECTRAL.

and, $L_f(Z, m', t')$ is the stellar variable to integrate, L_{bol} is the bolometric luminosity and $m(t)$ is the mass of star, which is alive at time t.

Finally, integrated variables are obtained by using :

$$< (f_1 - f_0) > = -2.5 \times log(\frac{< L_{f_1} >}{< L_{f_0} >}), \tag{11}$$

for indices and colors, and

$$< mag_f > = -2.5 \times log(< L_f >), \tag{12}$$

in the case of magnitude indices.

4. Evolution Models

4.1. Tests for the Evolutionary Synthesis Code

We have used instantaneous star-burst models to test and compare our code with others commonly used.

In the first part, we test colors and spectral indices; in the second part spectra for young and old populations.

4.1.1. Colors and Spectral Indices

For the first part we assume the next set of conditions:

An $\Phi(m_i) \propto m^\alpha$, with $\alpha = -2.35$, low mass limit, $m_l = 0.1$, and high mass limit, $m_h = 100.0$; and for SPECTRAL, we use Geneva tracks with normal mass loss rate.

1) In the first model we compare the evolution of colors at $Z = Z_\odot$ with those obtained from PEGASE97 (Fioc & Rocca-Volmerange 1997, FR) and GISSEL96 (Bruzual & Charlot 1993, BC). The Figure 3 shows this comparison.

We can see from the Figure 3, that there is a good agreement between the three models for colors. The dif-
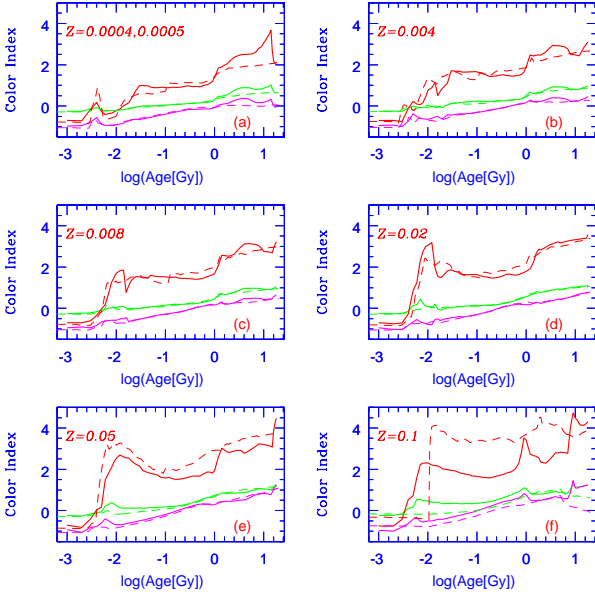
Fig. 4. Colors evolution as Figure 3 for star-bursts at different metallicities obtained with GISSEL96 (dashed lines) and SPECTRAL (full lines).

Fig. 5. Spectral indices evolution as the Figure 4 for star-bursts at different metallicities. GISSEL96 (dashed lines), and SPECTRAL (full lines).

ferences are due to the use of different spectral library (PEGASE97), or different stellar tracks (GISSEL96). In the same Figure 3 it is possible to see a pick in the $(V - K)$ color, around $log(Age[Gy]) = -1.0$, which is produced by thermal pulses generated by stars in range $(5.0 \leq m_i/M_\odot \leq 10.0)$, explained by FR. For a young population (around $log(Age[Gy]) = -2.0$) we can see an agreement between our model and that from FR in colors, and the agreement occurs with colors from BC in the inverse case when we compare old populations (around $log(Age[Gy]) = 1.0$).

2) In the second model we compare the same colors showed in Figure 3 for different metallicities with those obtained from GISSEL96 (Figure 4). In the same way we compare the evolution of two Lick indices H_β y Mg_b in Figure 5.

In the plot (a) of the Figure 4 we have compared models for the lowest metallicity reached linearly by our code with models at lowest metallicity in Padova tracks used by GISSEL96. There is a good agreement between models with different metallicities except for those at $Z = 0.1$ in plot (f) because the original tracks are incomplete.

In the case of indices, our models predict a flat and constant evolution for young populations (around $log(Age[Gy]) \leq -1.0$), while indices from BC present variations. The differences are due to they extend linearly to high temperatures the fitting functions (depending on T_{eff}, $log(M/H)$, and $log(g)$), which predict the value of each index, and we use the original fitting functions with temperature limit around 13,000 K. There is an agree-
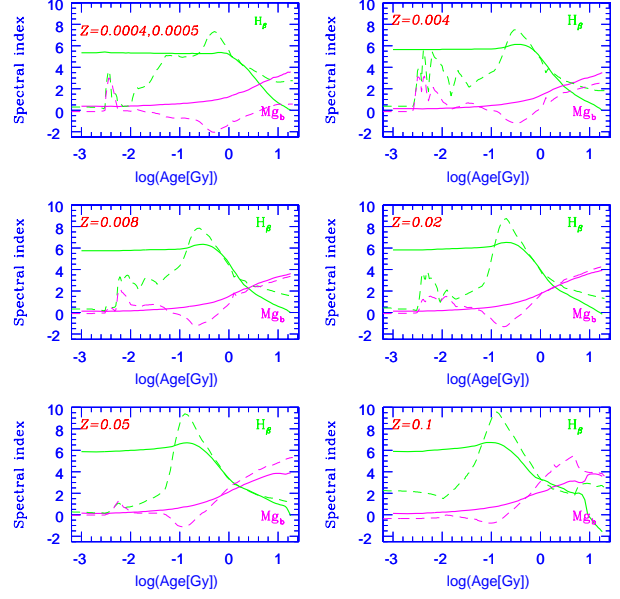
ment between both models for populations in the range of $log(Age[Gy]) > -1.0$.

4.1.2. Spectra

We have tested spectra in a different way. We have divided the test for two ranges, for young stellar populations and for old stellar populations. Both ranges were subdivided in three metallicities. We use instantaneous star-bursts as the star formation rate.

For **young populations** we assume the next set of conditions:

An $\Phi(m_i) \propto m^\alpha$, with $\alpha = -2.35$, low mass limit, $m_l = 1.0$, and high mass limit, $m_h = 100.0$, and for SPECTRAL we use Geneva tracks with high mass loss rate.

1) In the first model we compare our spectra with different ages in the range of $10^{-3} \leq t/Gy \leq 0.9$ at $Z = Z_\odot$ with spectra produced by STARBURST99 (Leitherer et al. 1999). Figure 6 shows quantitative differences taking the $log(L_{S99_k}/L_{S_k}) + 0.5k$ ($k = 1, 13$), where L_{S99} is the luminosity from STARBURST99's spectra and L_S from SPECTRAL. All models from STARBURST99 used here are without nebular emission.

There is a very good agreement, and it is comprehensive, because both of codes use the same spectra library and the same stellar tracks. There is a contribution in the UV part of spectra for ages at 3 and 5 My because the WR phases at that ages, that is the reason why the luminosity increase in UV part and the rate of luminosities between both sets of models is higher. The same features are not
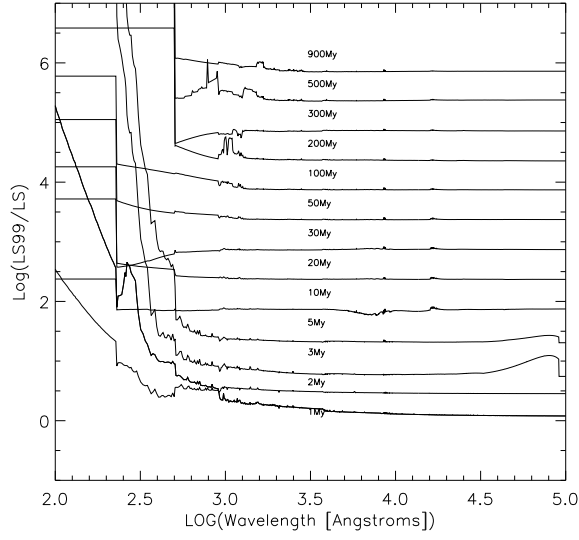
Fig. 6. Quantitative differences between our spectra and those from STARBURST99 at different ages, for a starburst at $Z = Z_{\odot}$.
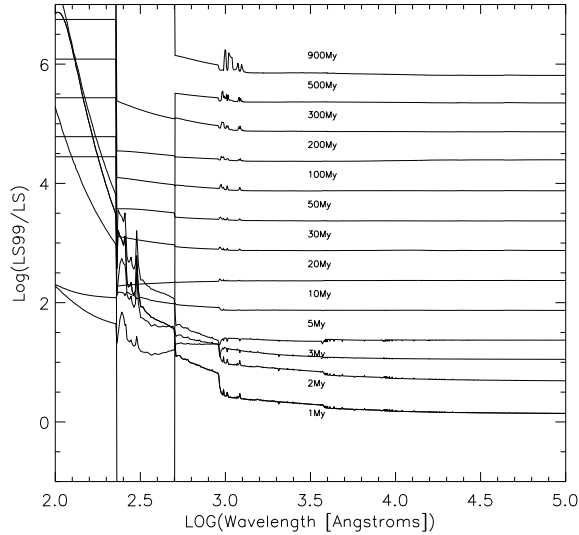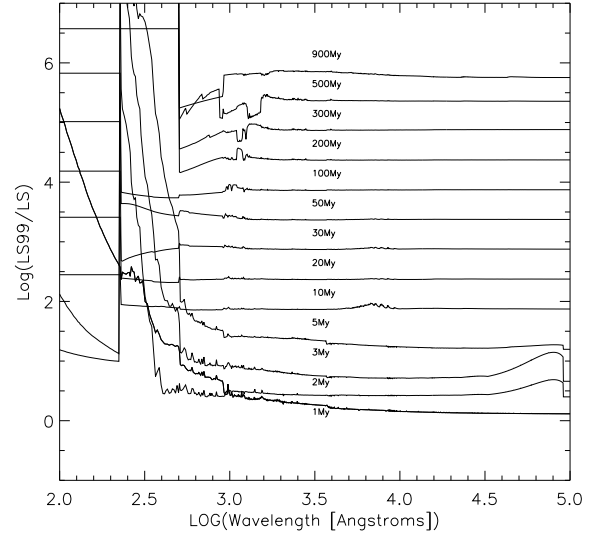

Fig. 7. Quantitative differences between our spectra and those from STARBURST99 at different ages, for a starburst at $Z = 0.001$.

visualized in our spectra because the library for massive stars with strong stellar winds are not considered in our spectra library. This increase of luminosity in UV part appears for STARBURST99 models at high metallicity, but not for low metallicity and the rate of luminosities is lower for low Z.

2) In the same way, the second model compares spectra with different ages at $Z = 0.001$. Figure 7 shows quantitative differences of these models.

Fig. 8. Quantitative differences between our spectra and those from STARBURST99 at different ages, for a starburst at $Z = 0.04$.

3) The final comparison is done for spectra at $Z = 0.04$. Figure 8 shows quantitative differences.

These three sets of models show a very good agreement with models from Leitherer et al. (1999). The same features for the case at $Z_{\odot}$ remain in models (2) and (3). This agreement shown in three different star-burst populations at different metallicities is present in the rest of metallicities of Geneva tracks as showed in Vázquez (2001).

For **old populations** we assume the next set of conditions:

An $\Phi(m_i) \propto m^{\alpha}$, with $\alpha = -2.35$, low mass limit, $m_l = 0.1$, and high mass limit, $m_h = 100.0$; and for SPECTRAL we use Geneva tracks with normal mass loss rate.

1) In the first model we compare our spectra with different ages in the range of $1.0 \leq t/Gy \leq 20.0$ at $Z = Z_{\odot}$ with spectra produced by GISSEL96 (BC). Figure 9 shows quantitative differences taking the $log(L_{G96_k}/L_{S_k}) + k$ $(k = 1, 6)$, where L_{G96} is the luminosity from GISSEL96's spectra and L_S from SPECTRAL.

It is easy to see some differences from Figure 9, which are due to the stellar tracks used for each code, Padova (GISSEL96) and Geneva (SPECTRAL), respectively. The considered spectral library is the same, but not the same version, which is a source of differences as well. The main differences are in the blue part of the spectra, where we find a contribution in UV due to old stars in phases like HB and planetary nebula predicted by additional stellar library used by GISSEL96, and there is not a counterpart in our models. Again, this is the reason why the rate of luminosities is higher for those models from GISSEL96.

2) In the same way, the second model compares spectra with different ages at $Z = 0.004$. Figure 10 shows quantitative differences of these models.
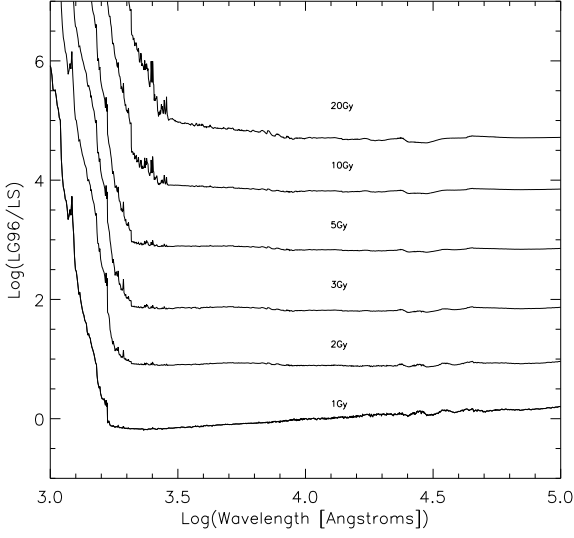
Fig. 9. Quantitative differences between our spectra and those from GISSEL96 at different ages, for a star-burst at $Z = Z_\odot$.
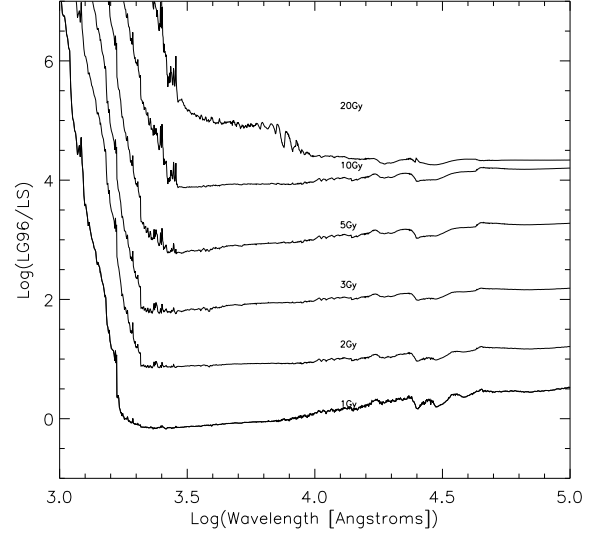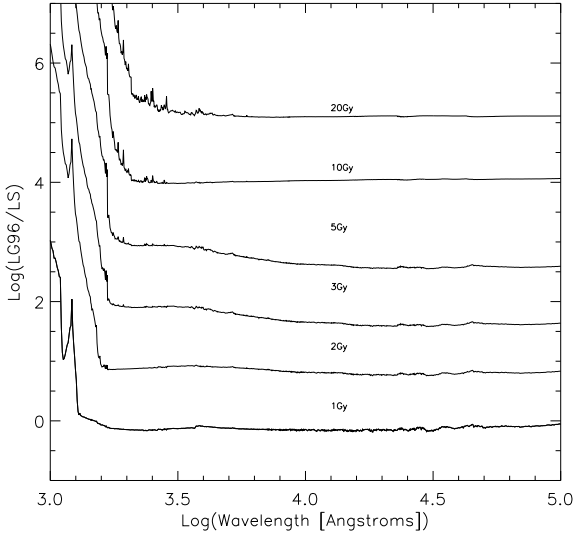

Fig. 10. Quantitative differences between our spectra and those from GISSEL96 at different ages, for a star-burst at $Z = 0.004$.

3) The final comparison is done for spectra at $Z = 0.05$. Figure 11 shows quantitative differences.

The features shown in models (2) and (3) are explained in the same form as those with $Z_\odot$. The rest of models at different metallicities are shown in Vázquez (2001).

4.2. Models for the irregular galaxy NGC 1560

Carigi, Colín & Peimbert (1999) discussed the chemical evolution of three irregular galaxies: NGC 1560, II

Fig. 11. Quantitative differences between our spectra and those from GISSEL96 at different ages, for a star-burst at $Z = 0.05$.

Zw 33 and a mean irregular galaxy. In the attempt to apply spectro-chemical evolution models to this three galaxies, we look for spectro-photometric measurements of these galaxies in the literature. In this work, we compute spectro-chemical evolution models only to NGC 1560 because: i) For NGC 1560 and II Zw 33 the nonbaryonic dark matter inside the Holmerg Radius is known, which constrains the chemical evolution models. ii) For NGC 1560, but nor for II Zw 33, neither the sample galaxies that form the mean irregular galaxy, there are photometric measurements to constrain the spectral models.

We have used close box models from Carigi, Colín & Peimbert (1999) updated with yields from Maeder (1992) and van den Hoek & Groenewegen (1997) to be consistent with stellar evolution models with normal mass loss rate used by our code. Chemical evolution models reproduce two constraints O/H abundance (Richer & McCall, 1995) and $\mu = M_{gas}/M_{total}$ (Walter et al. 1997, Broelis 1992). Three models with different ages and star formation rates to match the gas metallicity observed are not able to give us information about the age of star formation history. Colors of this galaxy may constrain the age if we use evolutionary synthesis.

These three chemical models results were used by our code to constrain the stellar population age which dominates the light in the irregular galaxy NGC 1560.

These models use the basic form for the IMF from Kroupa, Tout & Gilmore (1993), in the range of $0.01 \leq m_i/M_\odot \leq 120.0$ as follow:

$$\Phi(m_i) \sim \begin{cases} m_i^{-\alpha} & if \ \ 0.01 \leq m_i/M_\odot < 0.5, \\ m_i^{-2.2} & if \ \ 0.5 \leq m_i/M_\odot < 1.0, \\ m_i^{-2.7} & if \ \ 1.0 \leq m_i/M_\odot < 120.0 \end{cases} \qquad (13)$$

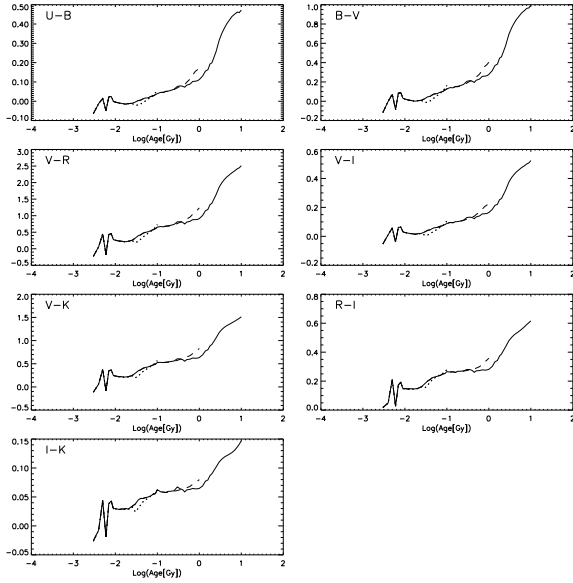**Fig. 12.** Broad band colors evolution for the three models at 0.1 Gy (dotted line), 1.0 Gy (dashed line), and 10.0 Gy (continuous line).

where α depends on chemical constraints and age of the model, and had three different values for every model:

$$\alpha = \begin{cases} -2.21 & \text{0.1 Gy Model} \\ -2.24 & \text{1.0 Gy Model} \\ -2.27 & \text{10.0 Gy Model} \end{cases} \qquad (14)$$

We use $\Phi(m_i)$, $\Psi(t)$, and $Z(t)$ from chemical models in SPECTRAL to produce a set of models. The set was produced by using tracks with the normal mass loss rate. Figure 12 shows the evolution of some broad band colors predicted for this galaxy.

The rest of broad band colors and Lick index for this set of models are shown in Vázquez (2001). The mean spectra produced for the models are shown in Figure 13.

The main goal in this work is to compare our predictions for this galaxy with those obtained observationally. For this galaxy we have obtained $(U - B)_0$ and $(B - V)_0$ from the de Vaucouleurs RC3, which are mean values. The evolution and the comparison is shown in Figure 14.

Figure 15 shows that the model which has a star formation age of 10.0 Gy fits in the best way the observations, it does not occur with younger models.

A better fit would be obtained if there were more colors, indices or the full spectrum in the literature.

5. Conclusions

We have extended the tracks from the Geneva group, producing two sets of tracks, one with high mass loss rate for masses in the range of $12.0 \leq m_i/M_\odot \leq 120.0$ and the other with normal mass loss rate in the range of $0.08 \leq m_i/M_\odot \leq 120.0$. These sets of tracks are complete
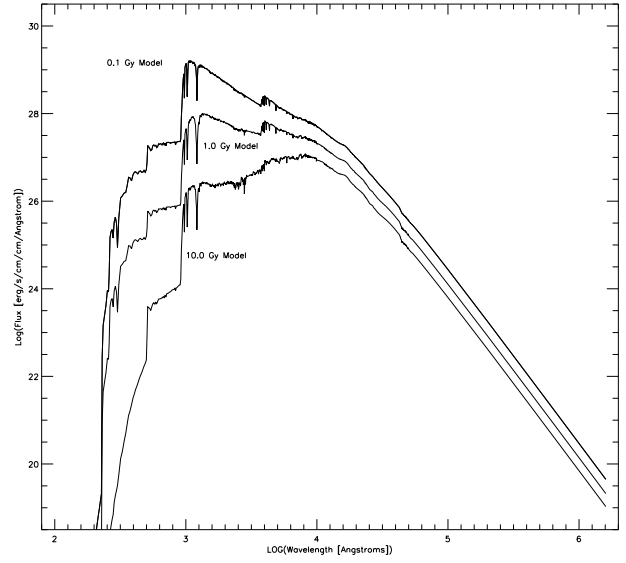

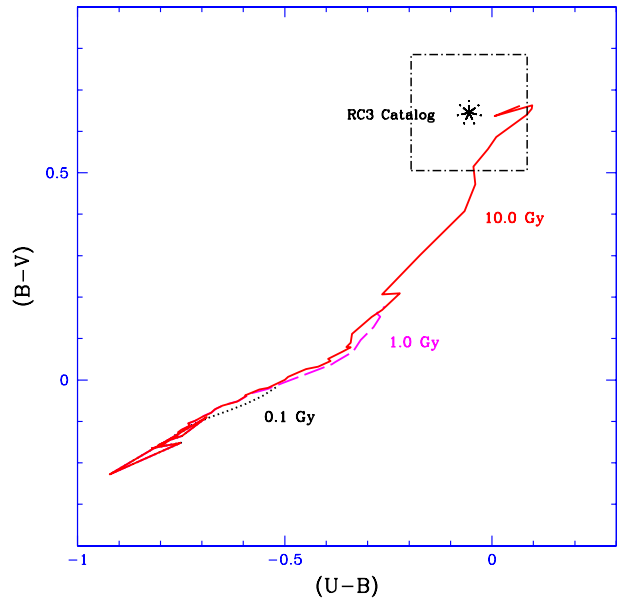**Fig. 13.** The spectra produced for the three models.

Fig. 14. $(U - B)$ vs. $(B - V)$ evolution for the three models are compared with observed values. Dotted line shows the 0.1 Gy model, dashed line for the 1.0 Gy model, and continuous line for the 10.0 Gy model. Box shows the error for the values from the literature.

and consistent for metallicities in the range $0.001 \leq Z \leq 0.04$, they cover phases from main sequence up to asymptotic giant branch in the range $0.8 \leq m_i/M_\odot \leq 120.0$, and pre-main sequence and main sequence for masses in $0.08 \leq m_i/M_\odot \leq 0.7$. Together with the spectral library, the code SPECTRAL is able to predict the spectral properties from stellar populations under a wide variety of conditions.
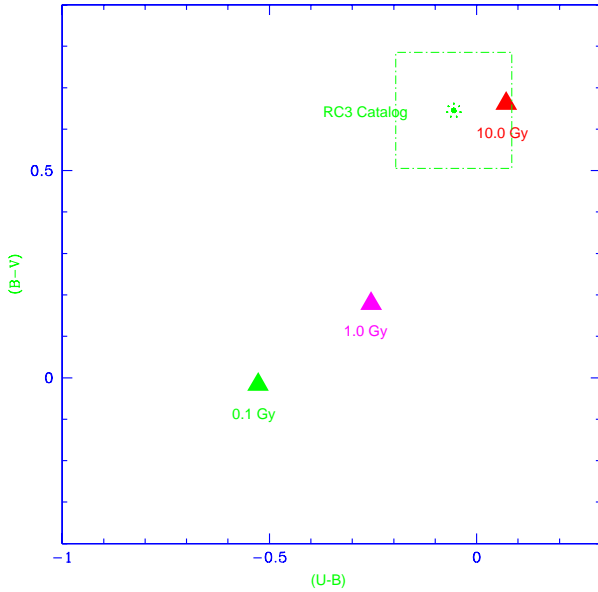
Fig. 15. $(U - B)$ vs. $(B - V)$ from models compared with values from the literature.

With this code, it is possible to build synthetic populations as the sophisticated chemical evolution models predict, as long as metallicity is in the range $0.001 \leq Z \leq 0.04$.

Results for star-burst evolution in broad band colors, spectral indices and spectra from our code fit very well with the same results obtained with other codes. SPECTRAL could be used in young stellar populations like in star-burst or blue galaxies, or stellar populations inside cores of AGN's. In the same way, the code could be used for old stellar populations like those in early type galaxies and all galaxy types in the middle of young and old stellar populations.

In applying just chemical models using observational constraints mentioned here for NGC 1560 it is not easy to distinguish what it is the age of the population. But using observed colors for this galaxy a spectro-chemical evolution model can be fitted and a population around 10 Gy and mean metallicity of stars $Z = 0.002$ are predicted with our model.

In the same way, from Figure 14, the evolution of colors for the 10.0 Gy model is possible to see that colors match the box error at 5 Gy. Furthermore, we might say that star formation history age for the mean stellar population is between [5.0,10.0 Gy], though we do not have chemical model for 5 Gy.

We have obtained success in reproducing the values for many simple star formation scenarios, and finally, we have matched very closely the values observed for two broad band colors in NGC 1560.

References

Broelis, A. 1992, A&A, 256, 19.

Bruzual, G. & Charlot S. 1993, ApJ 405, 538. (BC)

Carigi, L., Colín, P. & Peimbert, M. 1999, ApJ 514, 787.

Chabrier, G. & Baraffe, I. 1997, A&A, 327, 1039. (CB)

Charbonnel, C., Meynet, G., Meader, A., Schaller, G. & Schaerer, D. 1993, A&ASS, 101, 415. (III)

Charbonnel, C., Meynet, G., Meader, A. & Schaerer, D. 1996, A&ASS, 115, 339. (VI)

Charbonnel, C., Däpen, W., Schaerer, D., Bernasconi, P.A., Maeder, A., Meynet, G. & Mowlavi, N. 1999, A&ASS, 135, 405. (VIII)

de Vaucouleurs G., de Vaucouleurs A. Corwin H.G., et al., 1991, Third Reference Catalog of Bright Galaxies, Springer, New York.

Fioc, M. & Rocca-Volmerange, B. 1997, 326, 950. (FR)

González, J.J. 1993, PhD Thesis, University of California, Sta. Cruz.

Kroupa, P., Tout, C.A. & Gilmore, G. 1993, MNRAS, 262, 545.

Leitherer, C., Shaerer, D., Goldader, J.D., González Delgado, R.M., Robert, C., Kune, D.F., De Mello, D.F., Devost, D. & Heckman, T.M. 1999, ApJS, 123, 3.

Lejeune, T., Cuisinier, F. & Buser, R. 1997, A&ASS, 125, 229.

Lejeune, T., Cuisinier, F. & Buser, R. 1998, A&ASS, 130, 65.

Maeder, G. 1992, A&A, 264, 105.

Meynet, G., Maeder, G., Schaller, D., Schaerer, D. & Charbonnel, C. 1994, A&ASS, 103, 97. (V)

Mowlavi, N., Schaerer, D., Meynet, G., Bernasconi, P.A., Charbonnel, C. & Maeder, A. 1998, A&ASS, 128, 471. (VII)

Richer, M. & McCall, M. 1995, ApJ, 445, 659

Schaerer, D., Meynet, G., Meader, A. & Schaller, G. 1993a, A&ASS, 98, 523. (II)

Schaerer, D., Charbonnel, C., Meynet, G., Meader, A. & Schaller, G. 1993b, A&ASS, 102, 339. (IV)

Schaller, G., Schaerer, D., Meynet, G. & Maeder, A. 1992, A&ASS, 96, 269. (I)

Tinsley, B. 1972, A&A, 20, 383

van den Hoek, & Groenewegen, 1997, A&ASS, 123, 305.

Vazdekis, A., Casuso, E., Peletier, R. F. & Beckman, J. E. 1996, ApJS, 106, 307.

Vázquez, G.A. 2001, PhD Thesis, Instituto de Astronomía, UNAM.

Walter, F., Brinks, E., Duric, N. & Klein, U. 1997, AJ, 113, 2031.

Worthey, G., Faber, S.M., González J.J. & Burstein, D. 1994, ApJS, 94, 687.